Parametric Landau damping of space charge modes

Alexandru Macridin, Alexey Burov, Eric Stern, James Amundson, and Panagiotis Spentzouris

Fermilab, P.O. Box 500, Batavia, Illinois 60510, USA

Landau damping is the mechanism of plasma and beam stabilization; it arises through energy transfer from collective modes to the incoherent motion of resonant particles. Normally this resonance requires the resonant particle's frequency to match the collective mode frequency. We have identified an important new damping mechanism, *parametric Landau damping*, which is driven by the modulation of the mode-particle interaction. This reveals new possibilities for stability control through manipulation of both particle and mode-particle coupling spectra. We demonstrate the existence of parametric Landau damping in a simulation of transverse coherent modes of bunched accelerator beams with space charge.

I. INTRODUCTION

Landau damping (LD) [1] gives rise to the stabilization of collective modes in plasma and accelerator beams. The damping is caused by the energy transfer from the collective mode to the particles in resonance with the mode. The damping rate is, therefore, determined by the number of the particles capable of resonating with the mode. Conventionally, Landau damping requires the coherent resonance frequency to lie within the incoherent spectrum, i.e., to be located within the continuous frequency spectrum of the individual particles. Manipulation of the incoherent spectrum is often proposed as a mean to enhance stability; for example, the increase of the betatron tune spread in accelerators by using nonlinear magnets [2]. In this paper we discuss a new mechanism for Landau damping which occurs when the mode-particle coupling has an extended frequency spectrum. This mechanism reveals new possibilities for stability enhancement involving both particles' and the mode-particle coupling's spectra.

The novel Landau damping mechanism, which we call *parametric Landau damping*, is revealed by the numerical investigation of the transverse space charge modes in accelerator bunched beams at the coupling resonance, i.e., when the horizontal and the vertical tunes are close. In contrast with the usual Landau damping mechanism, the frequency of the LD-responsible particles, i.e., the particles which absorb the mode energy, have a wide spread and do not match the coherent frequency. This happens due to the

modulation of the mode-particle coupling by particle dependent oscillations with a wide frequency spread.

The transverse space charge modes in bunched beams, away from the coupling resonance were found analytically in Refs. [3–5]. Their intrinsic Landau damping in the strong space charge regime was suggested in Ref. [4]. Predicted damping rates were confirmed by numerical simulations [6–8].

The effect of linear coupling resonance on Landau damping was addressed by Metral in [9]. He showed that in the proximity of linear coupling resonance, the incoherent frequency spectrum from both transverse planes contributes to Landau damping. The collective mode transfers energy to the incoherent motions in both planes. Metral's mechanism is a shared damping between the transverse planes; a damping increase of the modes present in one plane implies a compensating decrease in the damping of the modes present in the other plane. In contrast, our mechanism is due to an oscillating mode-particle coupling implying additional conditions for the resonant energy transfer. Since our mechanism does not involve sharing, it is possible to enhance Landau damping for modes present in both planes. In our case the coupling between the transverse planes is produced by the space charge force, thus no linear terms are present. The main resonance is the fourth-order Montague resonance [10]. In our simulations the frequency of many LD-responsible particles does not match the coherent frequency. The enhancement of the damping rate cannot be explained by Metral's coupling resonance mechanism which requires the presence of resonant particles around the coherent frequency in the plane perpendicular to the mode.

A common feature of the particles trapped in the vicinity of resonance fixed points is the oscillation of their amplitudes. In the coupling resonance case the trapped particles are characterized by an oscillatory energy exchange between the transverse planes. Their transverse amplitudes

are oscillating with typical trapping frequencies. Since the mode-particle coupling is dependent on the particles' amplitudes, it is modulated by the trapping frequency. The resonance condition for Landau damping requires the particle frequency to equal the mode frequency shifted by the trapping frequency. Because the trapping frequencies are particle dependent, the frequencies of the LD-responsible particles may span a range equal to the one of the mode-particle coupling frequency spectrum.

We employ the Synergia accelerator modeling package [11,12] to simulate the propagation of a single Gaussian beam through a linear lattice. The modes are extracted from the transverse displacement density using the dynamic mode decomposition (DMD) technique [13–16]. DMD is a data driven algorithm used for modal analysis in both linear and nonlinear systems.

We compare the properties of the first space charge mode away and in the vicinity of the coupling resonance. We find that the Landau damping is larger in the latter case, while the frequency and the mode shape are nearly the same. By investigating the properties of the particles exchanging energy with the mode, we conclude that the off-resonance case well fits the conventional Landau damping scenario characterized by LD-responsible particles with an incoherent frequency spectrum at the coherent frequency. Around coupling resonance the damping enhancement is caused by the parametric Landau damping mechanism, a consequence of the modulated coupling between the mode and the trapped particles. The existence of the parametric Landau damping mechanism for the first space charge mode at coupling resonance is proven solely by numerical simulations of a bunch propagating through a lattice; no analytical model is assumed.

The paper is organized as follows. In Sec. II the mechanism of parametric Landau damping is formally introduced. In Sec. III the Landau damping mechanism of transverse space charge modes at coupling resonance is discussed. The details of the simulations are described in Sec. IV. The results of the simulations are presented in Sec. V, followed by discussions in Sec. VI. Summary and conclusions are given in Sec. VII. In Appendix A the calculation of tune shift and mode-particle coupling is discussed.

II. PARAMETRIC LANDAU DAMPING

The Landau damping mechanism results from the interaction of the collective mode with the individual particles. Using the simple harmonic oscillation approximation [17], the equation of motion for the particle i interacting with the mode $\bar{x}$ can be written as

$$\ddot{x}_i + \omega_i^2 x_i = -K_i \bar{x}(t), \tag{1}$$

where x_i represents the particle displacement, ω_i the particle frequency, K_i the mode-particle coupling and $\bar{x}(t)$ the collective mode.

In systems with conventional Landau damping, K is either time independent or its oscillation frequency is particle independent. The resonance condition is $\omega_i = \omega_c$, where ω_c is the $\bar{x}(t)$ frequency, i.e., $\bar{x}(t) \propto \exp(-i\omega_c t)$. The damping rate is proportional to the spectral density at the resonant frequency,

$$\lambda \propto \rho(\omega_c) = \sum_i \delta(\omega_i - \omega_c). \tag{2}$$

Nevertheless, as in the case addressed in this paper, it may happen that the mode-particle coupling is characterized by a frequency spectrum, i.e., $K_i(t) \propto \exp(-i\mu_i t)$ and μ_i is particle dependent. The resonance condition in this case is $\omega_i = \omega_c \pm \mu_i$. The damping rate is proportional to the number of particles which fulfill the resonance condition,

$$\lambda \propto h(\omega_c) = \sum_i \delta(\omega_c - \omega_i \pm \mu_i). \tag{3}$$

In this case the damping is determined by the interplay of both particles and mode-particle coupling spectra. We call this mechanism parametric Landau damping.

III. LANDAU DAMPING OF TRANSVERSE SPACE CHARGE MODES

For transverse space charge modes the equation of motion for the particle i can be written as (see Appendix A, Eq. (A16), [3–5,18])

$$\ddot{x}_i + \omega_0^2[Q_{0x} - \delta Q_x(z_i, J_{xi}, J_{yi})]^2 x_i$$
$$= -K(z_i, J_{xi}, J_{yi})\bar{x}(t, z_i), \tag{4}$$

where ω_0 is the angular revolution frequency and Q_{0x} is the bare betatron tune. The tune shift $\delta Q_x(z_i, J_{xi}, J_{yi}) \ll Q_{0x}$ and the mode-particle coupling $K(z_i, J_{xi}, J_{yi})$ are proportional to the longitudinal density and are dependent on the particle transverse actions, J_{xi} and J_{yi}, defined as

$$J_{xi} = \frac{x_i^2 + (\alpha_x x_i + \beta_x x_i')^2}{2\beta_x},$$
$$J_{yi} = \frac{y_i^2 + (\alpha_y y_i + \beta_y y_i')^2}{2\beta_y}, \tag{5}$$

where α_x, β_x, α_y and β_y are the lattice Twiss parameters.

The coherent driving term $\bar{x}(t, z_i)$ in Eq. (4) is the average displacement at the location where the particle is currently located and can be written as $\bar{x}(t, z_i) = e^{-i\omega_0 \nu t}\bar{x}[z_i(t)]$, where

$$\bar{x}(z) = \frac{\int dx dx' dy dy' du x \rho(x, x', y, y', z, u)}{\rho(z)}, \tag{6}$$

and ν being the mode tune [4]. Here z is the longitudinal position relative to the reference particle, $u = \frac{\delta p}{p}$ is the relative momentum spread, $\rho(x, x', y, y', z, u)$ is the density in 6D phase space and $\rho(z) = \int dx dx' dy dy' du \rho(x, x', y, y', z, u)$ is the longitudinal density. Unlike the situation described by Eq. (1), in Eq. (4) the uncoupled particle motion, the mode particle coupling and $\bar{x}$ are not characterized by a single frequency.

In order to address the Landau damping mechanism in the following part of this section we will investigate the conditions for resonant coupling between the particles and the collective mode. The explicit dependence of the tune shift δQ_x and the mode-particle coupling K on the particle's action coordinates is not important for this analysis.

In the off-resonance case, to a good approximation the particle transverse actions J_{xi} and J_{yi} are constants of motion and the time dependence of the tune shift $\delta Q_x(z_i, J_{xi}, J_{yi})$ is a consequence of the synchrotron motion given by $z_i(t) = a_i \cos(\omega_0 Q_s t + \varphi_i)$. Here a_i is the particle's longitudinal amplitude, Q_s is the synchrotron tune and φ_i is the particle's phase at $t = 0$. The tune shift $\delta Q_x(z_i, J_{xi}, J_{yi})$ for a Gaussian beam with the longitudinal density $\rho(z) = \exp(-z^2/2\sigma_z)$ can be expanded as

$$\delta Q_x[z_i(t), J_{xi}, J_{yi}]$$
$$= \delta Q_x[0, J_{xi}, J_{yi}] \exp\left(\frac{-z_i^2(t)}{2\sigma_z^2}\right)$$
$$= \delta Q_x[0, J_{xi}, J_{yi}] \exp\left(\frac{-[a_i \cos(\omega_0 Q_s t + \varphi_i)]^2}{2\sigma_z^2}\right)$$
$$= C_{0i} + \sum_{m=1}^{\infty} 2C_{mi} \cos[2m(\omega_0 Q_s t + \varphi_i)], \quad (7)$$

where

$$C_{mi} = \delta Q_x[0, J_{xi}, J_{yi}](-1)^m \exp\left(-\frac{a_i^2}{4\sigma_z^2}\right) I_m\left(\frac{a_i^2}{4\sigma_z^2}\right), \quad (8)$$

and I_m are the modified Bessel functions of the first kind. The tune shift contains a constant term which depends on the particle's longitudinal amplitude a_i and higher harmonics of $2Q_s$ terms. Since the mode-particle coupling $K(z_i, J_{xi}, J_{yi})$ is also proportional to the charge density $\rho(z)$, an analogous expansion is valid for the mode-particle coupling term

$$K[z_i(t), J_{xi}, J_{yi}] = K_{0i} + \sum_{m=1}^{\infty} 2K_{mi} \cos[2m(\omega_0 Q_s t + \varphi_i)]. \quad (9)$$

The mode $\bar{x}(t, z_i)$ frequency as seen by the particle i, is also influenced by the synchrotron motion. For that reason, the main tune of the first space charge mode is $\nu - Q_s$ and

not ν. This can be understood by considering the approximation $\bar{x}[z] \approx \sin[\pi z/4\sigma_z]$ [3,6] for the first space charge mode. The particle i sees the mode as

$$\bar{x}[t, z_i(t)] \approx e^{-i\omega_0 \nu t} \sin\left[\frac{\pi a_i \cos(\omega_0 Q_s t + \varphi_i)}{4\sigma_z}\right]$$
$$= e^{-i\omega_0 \nu t}\left[J_1\left(\frac{\pi a_i}{4\sigma_z}\right) \cos(\omega_0 Q_s t + \varphi_i)\right.$$
$$\left. + higher\ harmonics\right]. \quad (10)$$

Here J_1 is the Bessel function of the first kind and *higher harmonics* represent $(2n + 1)Q_s$ higher harmonic terms proportional to higher order Bessel functions. They are smaller in magnitude compared to the J_1 term.

From Eqs. (4), (7), (9), and (10) one can conclude that, in the off-resonance case, the main energy resonant exchange specific to the Landau damping mechanism between the first space charge mode and the particles takes place at the tune $\nu - Q_s$. Resonant exchanges at tunes distanced from $\nu - Q_s$ by harmonics of $2Q_s$ are also present, but we find that they play only a minor role in the Landau damping mechanism, as discussed in Sec. V.

In the off-resonance case the Landau damping is conventional, since the oscillation frequencies of the mode-particle coupling are particle independent [K contains a constant term and harmonics of $2Q_s$, see Eq. (9)]. The situation is different at the coupling resonance. Unlike the off-resonance case, in the proximity of the coupling resonance J_{xi} and J_{yi} are not constants of motion. In fact the sum $J_{si} = J_{xi} + J_{yi}$ is a constant of motion, while the difference $J_{di} = J_{xi} - J_{yi}$ oscillates around the stable point with the trapping frequency $\omega_{ti} = \omega_0 Q_{ti}$ [see Eq. (A42)]. The essential feature for the parametric Landau damping mechanism is that the particle dependent Q_{ti} modulates the mode-particle coupling. This becomes evident when the mode-particle coupling is written as [see Eq. (A54)]

$$K(z_i, J_{xi}, J_{yi}) = A(z_i, J_{si}) + B(z_i, J_{si}, J_{di})J_{di}. \quad (11)$$

The terms $A(z_i, J_{si})$ and $B(z_i, J_{si}, J_{di})$ as well as the tune shift $\delta Q_x(z_i, J_{si}, J_{di})$ depend on the beam shape and can be approximated analytically for certain cases. We discuss the calculation of the tune shift and the mode-particle coupling in Appendix A. In the Appendix A 2, to give an example, we calculate the particles' dynamics in the proximity of the coupling resonance stable point for a 2 dimensional (2D) Hamiltonian with a fourth order, rotationally symmetric transverse coupling term. Equation (A54) gives the mode-particle coupling in our example. A more general Hamiltonian describing the dynamics at coupling resonance, but without the presence of collective modes, was considered by Montague [10].

The equation of motion in the proximity of the coupling resonance is

$$\ddot{x}_i + \omega_0^2 Q_x^2(z_i, J_{si}, J_{di})x_i$$
$$= -A(z_i, J_{si})\bar{x}(t, z_i) - B(z_i, J_{si}, J_{di})J_{di}\bar{x}(t, z_i), \quad (12)$$

where $Q_x(z_i, J_{si}, J_{di}) = Q_{0x} - \delta Q_x(z_i, J_{si}, J_{di})$. Since J_{si} is a constant of motion, the coupling term $A\bar{x}$ is conventional. The term $BJ_d\bar{x}$ yields parametric Landau damping because it is modulated by oscillations with $\omega_0 Q_{ti}$ frequency. While in the former case the resonance condition is $\bar{Q}_{xi} = \nu - Q_s$, the $BJ_d\bar{x}$ term implies mode-resonant particles when $\bar{Q}_{xi} = \nu - Q_s - Q_{ti}$. Here $\bar{Q}_{xi}$ is the particle i main tune defined as the tune of the largest peak in the Fourier spectrum of $x_i(t)$. In principle the dependence of $B(z, J_s, J_d)$ on J_d yields resonant energy exchanges at frequencies spaced by harmonics of Q_t from the main parametric resonant condition, i.e., $\bar{Q}_{xi} = \nu - Q_s - Q_{ti} + nQ_{ti}$, but in our simulations we find these processes not to be significant.

The oscillations of J_d contribute not only to the parametric Landau damping but to the conventional one as well. The dependence of $Q_x(z_i, J_{si}, J_{di})$ in Eq. (12) on J_{di} yields satellite features spaced by harmonics of Q_{ti} in the incoherent spectrum. These satellites are resonant via $A\bar{x}$ coupling when their tune is equal to $\nu - Q_s$.

IV. SIMULATIONS

The simulations are done by employing SYNERGIA [11], a particle tracking code for beam dynamics in accelerators. The space charge effects are implemented in SYNERGIA using the second order split-operator method [19]. At every step, the electric field is calculated by solving the 3D Poisson equation with open boundary conditions numerically as described in [20].

The bunch is initially excited in the horizontal plane with the first space charge harmonic function. Space charge harmonics are the space charge modes of Gaussian beams in the strong space charge limit and were calculated analytically in Refs. [4,5]. The excitation amplitude is small enough to ensure linear damping regime and not to affect the particles' tune spectrum. The transverse displacement density,

$$X(z, u, s) = \frac{\int dx dx' dy dy' x\rho(x, x', y, y', z, u, s)}{\rho(z, u, s)}, \quad (13)$$

is calculated at every turn. Here s is the distance along the reference trajectory, and

$$\rho(z, u, s) = \int dx dx' dy dy' \rho(x, x', y, y', z, u, s) \quad (14)$$

is the density in the longitudinal phase space. The modes' shape, tune, and damping are extracted from $X(z, u, s)$

using the DMD technique. DMD [13–16] has been used for mode analysis in many fields such as fluid mechanics [21], neuroscience [22], and video streaming and pattern recognition [23]. An important advantage of this method is the direct calculation of mode dynamics, including shape, frequency, and growth/damping rates. Application of SYNERGIA and DMD to beam dynamics is described in detail in [8].

A lattice with the length 200 m made by 10 identical OFORODO (drift—focusing quad—drift—rf cavity—drift—defocusing quad—drift) cells is chosen. The difference between the actual phase advance and the smooth approximation phase advance nowhere exceeds 2% of the phase advance per cell. For the off-resonance case we take the bare betatron tune difference $Q_{0x} - Q_{0y} > \delta Q_{sc\,max}$ while at the coupling resonance $Q_{0x} = Q_{0y}.\delta Q_{sc\,max}$ is the space charge tune shift at the center of the bunch. The tunes in our simulations have values in the range typical for real circular accelerators, with $Q_s \ll Q_{0x}, Q_{0y}$. The majority of the simulations are done with $Q_{0x} = 2.322$ and $Q_s = 0.01$. We checked the robustness of our results for other values of the tunes, such as $Q_{0x} = 2.443$ and $Q_s = 0.005$. A proton beam with the energy corresponding to the relativistic factor $\gamma = 1.6$ is chosen. The chromaticity is zero. 10^8 macroparticles per bunch are used for the simulations. The beam distribution is longitudinally and transversely Gaussian with equal vertical and horizontal emittances, $\epsilon_x^{rms} = \epsilon_y^{rms} = 1$ mm $*$ mrad. The space charge parameter is defined as $q = \frac{\delta Q_{sc\,max}}{Q_s}$.

V. RESULTS

While the formalism described in Secs. II and III and Appendix A is useful for understanding the damping mechanism and interpreting the simulations, the results presented in this section are based only on the tracking simulations of a Gaussian beam through an OFORODO lattice, as described in Sec. IV.

The properties of the first space charge mode off-resonance and at coupling resonance are compared in Fig. 1. For intermediate and large space charge, $q \gtrsim 4$, the damping at coupling resonance is larger, as shown in Fig. 1(a). In the strong space charge regime, $10 \lesssim q \lesssim 20$, the damping at coupling resonance is larger by approximately a factor of 2. The relative enhancement increases slowly with q. However the precision of the simulation at large q is limited by the small value of the Landau damping, which becomes of the order of the error bars. The mode tune measured relative to the bare betatron tune, $\nu - Q_{0x}$, is nearly the same for both cases, see Fig. 1(b). The difference between the mode spatial shape in the two cases is also insignificant, as illustrated in Fig. 1(c) where the spatial overlap of the mode, $X_1(z, u)$, with the first space charge harmonic $Y_1(z)$ ($Y_1(z)$ is calculated in [4]),
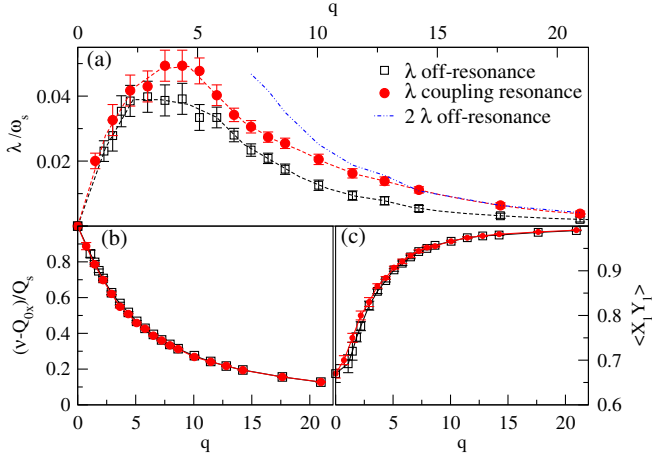
FIG. 1. Comparison between the off-resonance and the coupling resonance cases for the first space charge mode: (a) Landau damping rate $\frac{\lambda}{\omega_s}$ versus space charge parameter q, where $\omega_s = \omega_0 Q_s$ is the synchrotron frequency. For intermediate and strong space charge the damping is larger at the coupling resonance. (b) The mode tune ν at off-resonance and at coupling resonance are nearly the same. (c) The spatial overlap, Eq. (15), of the DMD extracted mode $X_1(z, u)$ with the space charge harmonic function $Y_1(z)$. The off-resonance and the coupling resonance mode shapes are nearly the same.

$$\langle X_1 Y_1 \rangle = \int X_1(z, u) Y_1(z) \rho(z, u) dz du, \qquad (15)$$

is plotted.

The off-resonance Landau damping mechanism can be understood within the typical paradigm. In Fig. 2(a) we plot the beam 2D tune footprint $\rho(Q_x, Q_y)$ defined as

$$\rho(Q_x, Q_y) = \sum_i |\tilde{x}_i(Q_x)|^2 |\tilde{y}_i(Q_y)|^2, \qquad (16)$$

where

$$\tilde{x}_i(Q_x) = \frac{1}{C_{xi}} \int x_i(s) e^{i\omega_0 Q_x s} ds \qquad (17)$$

is the Fourier transform of the particle i horizontal displacement $x_i(s)$. An analogous definition is used for $\tilde{y}_i(Q_y)$. Since the Landau damping is determined by the tune density and is insensitive to the particles' amplitude *per se*, the constant C_{xi} in Eq. (17) is used to normalize the spectral weight of each particle, Eq. (16), to one. As a consequence, the integrated $\rho(Q_x, Q_y)$ over the horizontal and the vertical frequencies is equal to the number of particles in the bunch. The space charge force shifts the particles' tunes to lower values. The tune depression is maximal at the bunch center, while the particles in the distribution tails have a much smaller tune shift. The satellite lines separated by $2Q_s$ are a consequence of the modulation of the tune shift with the particle's longitudinal position [as Eq. (7) predicts]. The particles directly
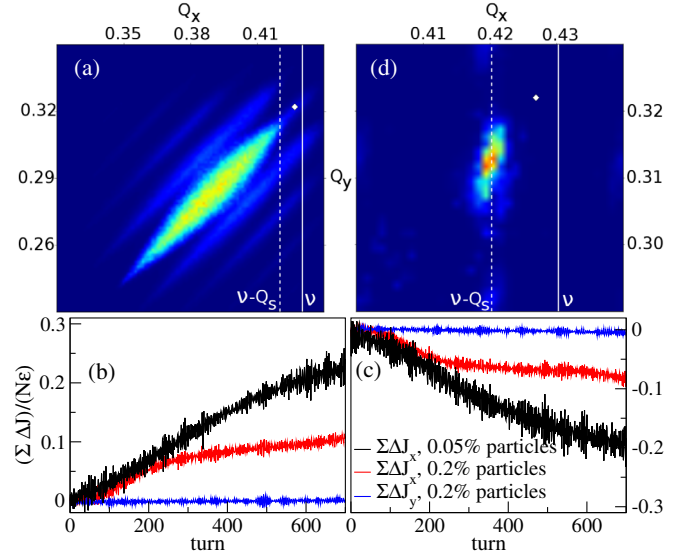

FIG. 2. (a) Bunch tune footprint at off-resonance for $q = 7.94$. The white dot corresponds to the bare betatron tunes. (b) $\sum_{i \in S} \Delta J_x = \sum_{i \in S} (J_{xi} - J_{xi\,\text{initial}})$ and $\sum_{i \in S} \Delta J_{yi} = \sum_{i \in S} (J_{yi} - J_{yi\,\text{initial}})$ of the 0.05% and 0.2% largest increasing energy particles versus turn number, normalized by the product of emittance and the number of the particles in the sum. (c) The same as (b) but for the largest decreasing energy particles. (d) Tune footprint for the 0.5% largest changing energy (increase and decrease) particles. The tunes are in the proximity of the coherent tune $Q_x = \nu - Q_s$. The color dimension scale in (a) and (d) differs by one order of magnitude.

responsible for the Landau damping are the ones which resonantly exchange energy with the mode. To select the LD-responsible particles we look for those having the largest change in their energy between the end and the beginning of the simulation. In Fig. 2(b) we plot

$$\sum_{i \in S} \Delta J_x = \sum_{i \in S} (J_{xi} - J_{xi\,\text{initial}}) \quad \text{and}$$
$$\sum_{i \in S} \Delta J_y = \sum_{i \in S} (J_{yi} - J_{yi\,\text{initial}}) \qquad (18)$$

where $J_{xi\,\text{initial}}$ and $J_{yi\,\text{initial}}$ represent the particle i actions at the beginning of the simulation. The notation S represents the subset of the 0.05% (black) or the 0.2% (red and blue) largest energy increase particles. A similar plot is shown in Fig. 2(c), but for the largest energy decrease particles. The values 0.05% and 0.2% are arbitrary chosen for the purpose of illustrating the properties of the LD-responsible particles. In the linear Landau damping theory, the energy of the LD-responsible particles increases linearly in a time interval $\delta t \approx 1/|\delta\omega|$, where $\delta\omega$ is the frequency difference between the particle and the mode. As seen from Fig. 2(b), the time where $\sum \Delta J_x$ is increasing linearly is larger when the number of the particles in the summation is smaller, since a larger number in the summation implies particles with larger $|\delta\omega|$. Note that the chosen particles increase or
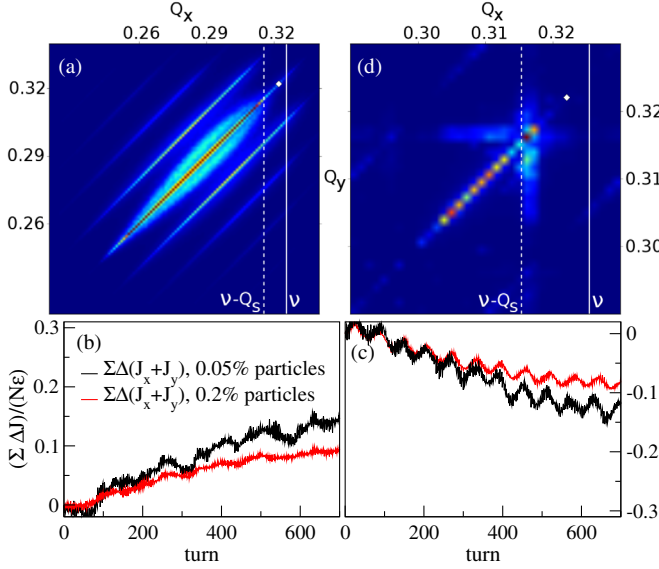
FIG. 3. (a) Bunch tune footprint at coupling resonance for $q = 7.94$. The white dot corresponds to the bare betatron tunes. (b) $\sum_{i \in S} \Delta J_{si} = \sum_{i \in S} (J_{si} - J_{si\,\text{initial}})$ of the 0.05% and 0.2% largest increasing energy particles versus turn number, normalized by the product of emittance and the number of the particles in the sum. (c) The same as (b) but for the largest decreasing energy particles. (d) Tune footprint for the 0.5% largest changing energy (increase and decrease) particles. Large part of the spectral weight is along the resonance line $2Q_x - 2Q_y = 0$, with the horizontal tune well below $\nu - Q_s$. The color dimension scale in (a) and (d) differs by one order of magnitude.

decrease their action only in the horizontal plane, i.e., the plane where the mode is present. The 2D tune footprint of the 0.5% largest-energy changing particles (both increasing and decreasing) is shown in Fig. 2(d). As expected, since these particles are mode-resonant, their horizontal tune is in the vicinity of $\nu - Q_s$. Notice that higher $\nu - (2n + 1)Q_s$ harmonics spectral features do not appear to be significant in the tune footprint of the LD-responsible particles.

The spectral properties of the LD-responsible particles at the coupling resonance do not fit the typical Landau damping paradigm. The beam 2D tune footprint in Fig. 3(a) displays enhanced spectral weight along the coupling resonance line $2Q_x - 2Q_y = 0$, consequence of resonance trapping [in agreement with Eqs. (A45) and (A46)]. Satellite lines corresponding to the $2Q_s$ harmonics can be observed too. We use the same largest energy change criterion to select the LD-responsible particles. Unlike the off-resonance case, the horizontal and vertical actions exhibit nonmonotonic change with turn number, since in the proximity of coupling resonance their magnitude oscillates between the planes. However, the transverse action sum J_s of the LD-responsible particles displays a monotonic increase (decrease), as shown in Fig. 3(b) [Fig. 3(c)]. The interesting fact which points to a parametric damping mechanism is that the tune of most of these large energy changing particles is not in the vicinity of $\nu - Q_s$ as
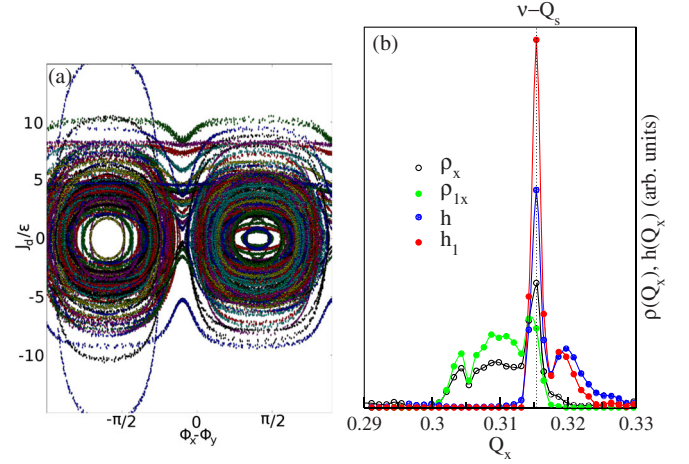
one would expect for LD-responsible particles. As shown in Fig. 3(d), there is a large spectral weight on the coupling resonance line which extends well below $Q_x = \nu - Q_s$.

Most of the large changing energy particles are trapped in resonance islands, as can be seen in Fig. 4(a) where the Poincare plots, J_{di} versus $\Phi_{xi} - \Phi_{yi}$ for $i \in S$, are shown. The phase coordinates are defined as

$$\Phi_{xi} = \arctan\left(-\frac{\alpha_x x_i + \beta_x x_i'}{x_i}\right),$$

$$\Phi_{yi} = \arctan\left(-\frac{\alpha_y y_i + \beta_y y_i'}{y_i}\right). \tag{19}$$

The Landau damping is, therefore, strongly influenced by the J_d oscillations characterizing the coupling resonance trapped particles. The trapping frequency, $\omega_0 Q_{ti}$, of the LD-responsible particles is determined from the Fourier spectrum of $J_{di}(s)$.

The Q_t satellites in the particles' tune spectra contribute to the spectral weight at the mode coherent tune $\nu - Q_s$ by $\approx 20\%$–25%. This contribution favors the conventional damping mechanism via the $A\bar{x}$ coupling [see Eq. (12)]. To estimate the Q_t satellites' spectral weight we compare the horizontal tune density

$$\rho_x(Q) = \sum_{i \in S} \rho_{xi}(Q) = \sum_{i \in S} |\tilde{x}_i(Q)|^2 \tag{20}$$

and the one-tune-per-particle density

$$\rho_{1x}(Q) = \sum_{i \in S} \rho_{1xi}(Q) = \sum_{i \in S} \delta(Q - \bar{Q}_{xi}). \tag{21}$$

FIG. 4. Coupling resonance, $q = 7.94$. (a) Poincare plots, J_d versus $\Phi_x - \Phi_y$, for randomly selected particles belonging to the 0.5% largest changing energy particles. Most of these particles are trapped in the resonance islands. (b) The horizontal tune density $\rho(Q_x)$ (black), the Q_t shifted tune density $h(Q_x)$ (blue) and the one-tune-per-particle tune density $\rho_1(Q_x)$ (green) with the corresponding Q_t shifted tune density $h_1(Q_x)$ for the 0.5% largest changing energy particles. $h(Q_x)$ and $h_1(Q_x)$ are strongly peaked at the resonant mode tune $Q_x = \nu - Q_s$, showing mode-particle resonance via the $BJ_d\bar{x}$ term [see Eq. (12)].

The sums in Eqs. (20) and (21) are restricted only to the number of the selected particles with the largest energy change. $\bar{Q}_{xi}$ is the tune of the largest spectral peak in the Fourier spectrum $|\tilde{x}_i(Q)|$. Unlike ρ_x, where all spectral features are present, ρ_{1x} assumes that every particle is characterized only by its main tune. The spectral weight difference between ρ_x and ρ_{1x} at $\nu - Q_s$ measures the satellites contribution to the $A\bar{x}$ damping mechanism. In Fig. 4(b) ρ_x and ρ_{1x} for the 0.5% largest changing energy particles are shown. Besides the peak at $\nu - Q_s$, a broad spectral feature at smaller frequency, unfavorable to the $A\bar{x}$ damping mechanism, is observed in both ρ_x and ρ_{1x}.

The other contribution of the J_d oscillations to the damping is via the $BJ_d\bar{x}$ term. The resonance condition is $Q_{xi} + Q_{ti} = \nu - Q_s$. We define $h(Q)$ as the tune density obtained by shifting each particle's horizontal tune by Q_{ti}, such

$$h(Q) = \sum_{i\in S} h_i(Q) = \sum_{i\in S} \int \rho_{Jdi}(Q')\rho_{xi}(Q - Q')dQ'$$
$$\approx \sum_{i\in S} \rho_{xi}(Q - Q_{ti}), \tag{22}$$

where $\rho_{Jdi}(Q) = |\tilde{J}_{di}(Q)|^2$ is the Fourier spectrum of $J_{di}(s)$. We define $h_1(Q)$ by replacing ρ_{xi} with ρ_{1xi} in Eq. (22). As shown in Fig. 4(b), both $h(Q)$ and $h_1(Q)$ are strongly peaked at the coherent frequency $\nu - Q_s$ and do not display the broad spectral feature seen in $\rho_x(Q)$ and $\rho_{1x}(Q)$ below $\nu - Q_s$. In fact the particles with the tune forming the broad spectral feature of $\rho_{1x}(Q)$ have the main tune $\bar{Q}_{xi} \approx \nu - Q_s - Q_{ti}$, i.e., the tune required for resonance with the $BJ_d\bar{x}$ coupling term. The broad feature seen in $h(Q)$ $[h_1(Q)]$ spectrum above $\nu - Q_s$ corresponds to the spectral weight at $\nu - Q_s$ in the tune density $\rho_x(Q)$ $[\rho_{1x}(Q)]$ when shifted with particle dependent Q_{ti}.

Compared to the off-resonance case, at coupling resonance the mode-particle coupling term $BJ_d\bar{x}$ allows a larger number of particles to participate to the damping process. The conventional coupling does not favor particles with small longitudinal amplitudes, since they have a large tune shift which excludes them from the resonant exchange process with the mode. However, this impediment is not so restrictive for the resonant exchange via the $BJ_d\bar{x}$ term, since the trapping frequency Q_t is proportional to the charge density, thus also being large for small longitudinal amplitude particles and partially compensating for the large tune shift.

VI. DISCUSSIONS

In our simulations we choose the initial amplitude excitation of the space charge mode to be small, of order of $10^{-3}\sigma_x$, where σ_x is the beam horizontal rms size. As a consequence, the change in the beam shape and size are of the same order of magnitude. In a good approximation the
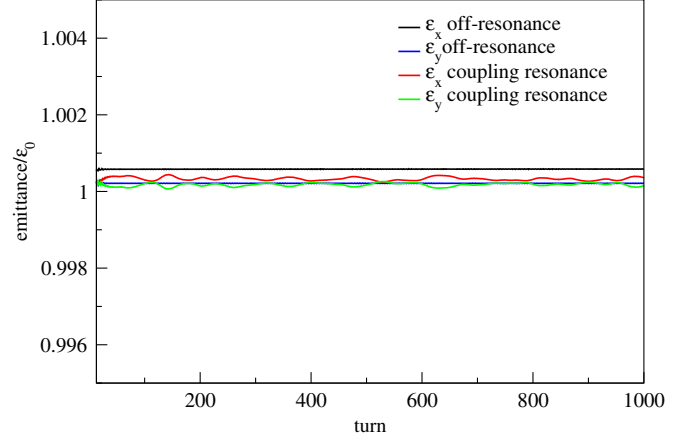

FIG. 5. The horizontal and the vertical emittances versus the turn number for the off-resonance and the coupling resonance cases for $q = 7.94$. The emittances are nearly constant, the relative change being smaller than 5×10^{-4}.

beam size is constant. One may wonder about beam shape at the coupling resonance case, which, in general, is associated with the Montague's emittance exchange between transverse planes [10]. The Montague's emittance exchange occurs when the horizontal and the vertical emittances differs significantly from each other. In our case the initial beam distribution is chosen such that $\epsilon_x = \epsilon_y \equiv \epsilon_0$, and the emittance exchange is negligible. While at the particle level the coupling resonance is characterized by amplitude exchange between the transverse planes, the overall beam distribution changes very little. In Fig. 5 we plot the transverse emittances versus the turn number, both at the coupling resonance and in the off-resonance case. The relative change of the horizontal and the vertical emittances are smaller than 5×10^{-4}.

While our simulations show enhanced damping at the coupling resonance it is important to address the damping behavior when moving away from this point. We investigate the damping as a function of the bare betatron tunes difference $\Delta Q_0 = Q_{0x} - Q_{0y}$. In Fig. 6 we plot the Landau damping of the horizontal first space charge mode versus $\Delta Q_0 / Q_s$ for different values of the space charge parameter and the synchrotron tune. The width of the enhanced damping region scales linearly with the space charge tune shift, $W \approx 0.3 Q_{sc\,max}$, where W is defined as the width at half maximum. The enhanced damping region is asymmetric with respect the to $\Delta Q_0 = 0$, extending predominantly ($\approx 80\%$) on the negative side of ΔQ_0. We notice two maxima of the damping rate in the enhanced damping region. One is at coupling resonance $\Delta Q_0 = 0$ and the other at $-\Delta Q_0 = M$. The value of M increases slightly increasing q as shown in the inset of Fig. 6. Our preliminary results indicate that the $-\Delta Q_0 = M$ maximum and the asymmetry of the enhanced damping region are related to a different modulation of the mode-particle coupling. Those results will be addressed in detail in a future publication.
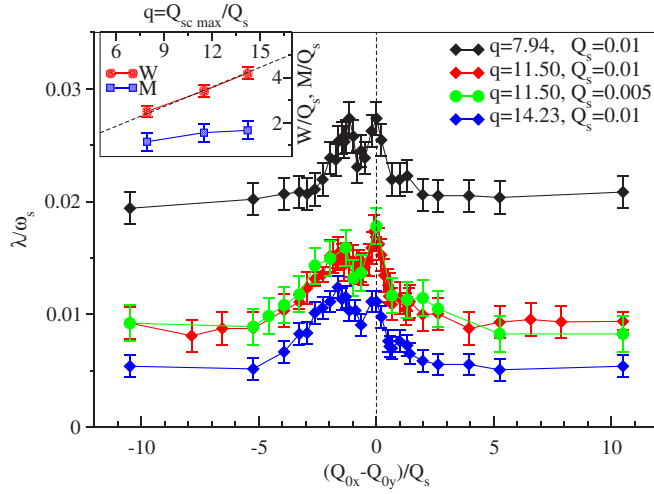
FIG. 6. Landau damping rate $\frac{\lambda}{\omega_s}$ of the horizontal first space charge mode versus $\Delta Q_0/Q_s = (Q_{0x} - Q_{0y})/Q_s$ for different values of the space charge parameter q and the synchrotron tune Q_s where $\omega_s = \omega_0 Q_s$ is the synchrotron frequency. The width of the enhanced damping region in the proximity of coupling resonance W, defined at half maximum, scales linearly with the space charge tune shift, $W \approx 0.3 Q_{sc\,\max}$, as shown in the inset. The enhanced damping region is asymmetric with respect to the to $\Delta Q_0 = 0$, extending predominantly on the negative side of ΔQ_0. Two maxima of the damping rate can be noticed, one at $\Delta Q_0 = 0$ and the other one at $\Delta Q_0 \approx -M$.

VII. CONCLUSIONS

A novel Landau damping mechanism, driven by the modulation of the mode-particle coupling is introduced. Numerical simulations using SYNERGIA with the DMD method show the existence of this mechanism in bunched beams in the proximity of coupling resonance. The properties of the first space charge mode are calculated for a Gaussian bunch propagating through an OFORODO lattice. The off-resonance and the coupling resonance cases are compared. While the space charge mode's tune and shape are nearly the same, the Landau damping is approximately a factor of 2 larger at coupling resonance in the strong space charge regime. In the off-resonance case the damping mechanism can be understood within the conventional paradigm. The damping is caused by the resonant energy exchange between the mode and the particles with an incoherent tune equal to the mode's tune shifted by Q_s. At coupling resonance a large number of particles are trapped around the stable points. Their transverse actions are oscillating with a particle dependent trapping frequency $\omega_0 Q_t$. The spectral properties of the trapped particles with large energy exchange reveal that their tune is additionally shifted from the mode's coherent tune by Q_t, supporting the parametric Landau damping mechanism.

APPENDIX: TUNE SHIFT AND MODE-PARTICLE COUPLING

The space charge induced tune shift and the coupling of the space charge collective modes to the incoherent motion of the particles are dependent on the particles amplitudes. The interpretation of our numerical results is based on this assumption. For realistic beams it is difficult to derive analytical expressions for the tune shift and the mode-particle coupling. In this appendix we calculate these expressions using a simply model. Despite the simplifying assumptions, the derivations provide insight on the dependence of the tune shift and the mode-particle coupling on the particles properties.

We consider a 2D model with transverse degrees of freedom

$$H = \frac{p_x^2}{2} + \frac{1}{2}\omega_{0x}^2 x^2 + \frac{p_y^2}{2} + \frac{1}{2}\omega_{0y}^2 y^2 + V(x,y), \quad (A1)$$

were $V(x,y)$ is the space charge interaction part of the Hamiltonian.

1. Off-resonance case

We will introduce two different approaches for particle's frequency calculation. In the first approach one writes the Hamiltonian in the canonical action-angle coordinates

$$H = \omega_{0x} J_x + \omega_{0y} J_y + V(J_x, J_y, \Phi_x, \Phi_y), \quad (A2)$$

where

$$x = \sqrt{\frac{2J_x}{\omega_{0x}}} \sin \Phi_x, \qquad p_x = \sqrt{2J_x \omega_{0x}} \cos \Phi_x. \quad (A3)$$

Analogous transformations are used for y and p_y. Since the space charge potential contains only terms with even powers of x and y, it can be written as

$$V(J_x, J_y, \Phi_x, \Phi_y)$$
$$= V_0(J_x, J_y) + V_1(J_x, J_y, \cos 2m\Phi_x, \cos 2n\Phi_y), m, n > 0.$$
$$(A4)$$

V_1 contains only high harmonics terms proportional to $\cos 2m\Phi_x$ and/or $\cos 2n\Phi_y$. Away from resonances (see Appendix A 2 for a discussion of the coupling resonance), the contribution of these terms averages to zero in time. V_1 can be neglected in the first order of perturbation theory. The particle's horizontal frequency is given by

$$\omega_x = \dot{\Phi}_x = \frac{\partial(H_0 + V_0)}{\partial J_x} = \omega_{0x} + \frac{\partial V_0}{\partial J_x}. \qquad (A5)$$

The frequency shift is

$$\delta\omega_x(J_x, J_y) = \omega_{0x} - \omega_x = -\frac{\partial V_0}{\partial J_x}(J_x, J_y). \qquad (A6)$$

Analogous equations can be written for the vertical frequency.

The second approach for the particle's frequency calculation starts from the equation of motion and is based on the Lindstedt-Poincare perturbation theory [24] for nonlinear equations. The horizontal displacement obeys

$$\ddot{x} + \omega_{0x}^2 x = F(x, y), \qquad (A7)$$

where

$$F(x, y) = -\frac{\partial V}{\partial x}(x, y) \qquad (A8)$$

is the space charge force considered to be a perturbation. In the first order of perturbation theory, only the terms in $F(x, y)$ which oscillate with a frequency close to ω_x are relevant for the particle dynamics. To isolate these terms we write x and y in the action-angle coordinates. $F(x, y)$ contains terms with odd powers of x and even powers of y and it can be written as

$$F(x, y) = F_0(J_x, J_y) \sin\Phi_x$$
$$+ F_1(J_x, J_y, \sin(2m + 1)\Phi_x, \cos 2n\Phi_y)$$
$$m, n > 0. \qquad (A9)$$

F_1 can be neglected since it contains only higher harmonics of $\omega_x = \dot{\Phi}_x$. Equation (A7) reduces to

$$\ddot{x} + \left(\omega_{0x}^2 - F_0(J_x, J_y)\sqrt{\frac{\omega_{0x}}{2J_x}}\right)x = 0, \qquad (A10)$$

and the horizontal tune shift is

$$\delta\omega_x(J_x, J_y) = F_0(J_x, J_y)\frac{1}{2\sqrt{2J_x\omega_{0x}}}. \qquad (A11)$$

Using Eqs. (A3) and (A8) one can check that Eq. (A6) and Eq. (A11) agree with each other.

To estimate the mode-particle coupling we will use the equation of motion. We consider a transverse mode which displaces the beam center infinitesimally by $\bar{x}$. Assuming the rigid-slice approximation, the space charge potential in this case is

$$V(x - \bar{x}, y) = V(x, y) - \frac{\partial V(x, y)}{\partial x}\bar{x}. \qquad (A12)$$

The equation of motion reads

$$\ddot{x} + \omega_{0x}^2 x = F(x, y) - \frac{\partial F}{\partial x}(x, y)\bar{x}. \qquad (A13)$$

The mode-particle coupling is given by the last term in Eq. (A13). In order to address the Landau damping mechanism, one has to investigate the parts in the $\frac{\partial F}{\partial x}(x, y)\bar{x}$ term which are in resonance with the particle displacement x. Let us assume in this section that the mode frequency ω_c is close to the particle's one ω_x, as it happens for the conventional Landau mechanism. Since $\frac{\partial F}{\partial x}(x, y)$ contains only even powers of x and y one can write

$$\frac{\partial F}{\partial x}(x, y) = G_0(J_x, Jy) + G_1(J_x, J_y)\cos 2\Phi_x$$
$$+ G_2(J_x, J_y, \cos 2m\Phi_x, \cos 2n\Phi_y)$$
$$m, n > 0. \qquad (A14)$$

Neglecting the high harmonics, the equation of motion can be written as

$$\ddot{x} + [\omega_{0x} - \delta\omega_x(J_x, J_y)]^2 x$$
$$\approx -G_0(J_x, Jy)\bar{x} + \frac{M}{2}G_1(J_x, J_y)\sin(2\Phi_x - \omega_c t). \qquad (A15)$$

Here M is the mode amplitude, $\bar{x} = M\sin\omega_c t$, and $\delta\omega_x(J_x, J_y)$ is given by Eq. (A11). Since $\sin(2\Phi_x - \omega_c t) \approx \sin(\omega_c t)$ when $\omega_c \approx \omega_x$ and the oscillations of x and $\bar{x}$ are in phase [25], one can write the equation of motion as

$$\ddot{x} + [\omega_{0x} - \delta\omega_x(J_x, J_y)]^2 x = -K(J_x, J_y)\bar{x}, \qquad (A16)$$

with the mode-particle coupling given by

$$K(J_x, J_y) = G_0(J_x, J_y) - \frac{1}{2}G_1(J_x, J_y). \qquad (A17)$$

We will end this section with an example. Let us consider a space charge potential

$$V(x) = \alpha x^4. \qquad (A18)$$

This is not a realistic potential but can be viewed as a term in the Taylor's expansion of the real potential. The space charge force is

$$F(x) = -4\alpha x^3 = -4\alpha \frac{2J_x}{\omega_{0x}} \sqrt{\frac{2J_x}{\omega_{0x}}} \sin^3 \Phi$$

$$= -4\alpha \frac{2J_x}{\omega_{0x}} \sqrt{\frac{2J_x}{\omega_{0x}}} \left(\frac{3}{4} \sin \Phi_x - \frac{1}{4} \sin 3\Phi_x \right). \quad (A19)$$

Therefore

$$F_0(J_x) = -\alpha \frac{6J_x}{\omega_{0x}} \sqrt{\frac{2J_x}{\omega_{0x}}}, \quad (A20)$$

and according to Eq. (A11) the tune shift is

$$\delta\omega_x(J_x) = -3\alpha \frac{J_x}{\omega_{0x}^2}. \quad (A21)$$

For the mode-particle coupling we have

$$\frac{\partial F}{\partial x}(x, y) = -12\alpha x^2 = -12\alpha \frac{J_x}{\omega_{0x}}(1 - \cos 2\Phi_x), \quad (A22)$$

implying

$$K(J_x) = -18\alpha \frac{J_x}{\omega_{0x}} = 3 \times 2\omega_{0x} \delta\omega_x(J_x). \quad (A23)$$

The factor of 3 in front of the right-hand side (r.h.s.) of the Eq. (A23) arises from the derivative of $F(x, y)$ with respect to x. A space charge force term $F(x) \propto x^{2n+1}$, implies $K(J_x) = (2n + 1) \times 2\omega_{0x} \delta\omega_x(J_x)$. In the linear regime where $F(x) \propto x$, valid for small amplitude oscillations, $K(J_x) = 2\omega_{0x} \delta\omega_x(J_x)$.

Note that Eq. (4) proposed to describe the particles motion in Sec. III, is a generalization of Eq. (A16) to include longitudinal degrees of freedom.

2. Transverse coupling resonance for round beams

The resonance effects on beam particles dynamics are treated extensively in the literature. However the question of how the resonance effects can influence the mode-particle coupling and implicitly the Landau damping mechanism has not been addressed. In this section, using a simplified space charge potential, we will discuss the mode-particle coupling in the proximity of transverse coupling resonance given by $2\omega_x - 2\omega_y = 0$.

To illustrate the calculation of tune shift and mode-particle coupling near coupling resonance we consider an example where the space charge potential is rotationally symmetric and given by

$$V(x, y) = \alpha(x^2 + y^2)^2. \quad (A24)$$

In the proximity of the coupling resonance it is easier to calculate the particles dynamics with a Hamiltonian formalism than by using the equation of motion. For the calculation of the frequency shift we transform the Hamiltonian to action-angle coordinates

$$H = \omega_{0x}J_x + \omega_{0y}J_y + \frac{3\alpha}{2}\left(\frac{J_x^2}{\omega_{0x}^2} + \frac{J_y^2}{\omega_{0y}^2}\right)$$

$$+ 2\alpha \frac{J_x J_y}{\omega_{0x}\omega_{0y}}\left(1 + \frac{1}{2}\cos(2\Phi_x - 2\Phi_y)\right). \quad (A25)$$

We neglect the high harmonics terms, as discussed in Sec. A 1. Assuming proximity of the coupling resonance the term proportional to $\cos(2\Phi_x - 2\Phi_y)$ is retained.

We proceed with a canonical transformation using the generating functional

$$F(\Phi_x, \Phi_y, I_x, I_y) = (\Phi_x - \bar{\omega}t)I_x + (\Phi_y - \bar{\omega}t)I_y, \quad (A26)$$

with $\bar{\omega} = \frac{1}{2}(\omega_{0x} + \omega_{0y})$. It leads to the Hamiltonian

$$\tilde{H} = \Delta\omega(-I_x + I_y) + \frac{3\alpha}{2}\left(\frac{I_x^2}{\omega_{0x}^2} + \frac{I_y^2}{\omega_{0y}^2}\right)$$

$$+ 2\alpha \frac{I_x I_y}{\omega_{0x}\omega_{0y}}\left(1 + \frac{1}{2}\cos(2\varphi_x - 2\varphi_y)\right), \quad (A27)$$

where

$$\Delta\omega = \frac{1}{2}(\omega_{0y} - \omega_{0x}) \quad (A28)$$

$$\varphi_x = \Phi_x - \bar{\omega}t, \qquad J_x = I_x \quad (A29)$$

$$\varphi_y = \Phi_y - \bar{\omega}t, \qquad J_y = I_y \quad (A30)$$

$$\tilde{H} = H - \bar{\omega}(I_x + I_y). \quad (A31)$$

A subsequent canonical transformation using the generating functional

$$F(\varphi_x, \varphi_y, J_s, J_d) = \frac{1}{2}J_s(\varphi_x + \varphi_y) + \frac{1}{2}J_d(\varphi_x - \varphi_y), \quad (A32)$$

leads to the Hamiltonian

$$H = -\Delta\omega J_d + \alpha[a_s J_s^2 + a_d J_d^2 + b J_s J_d$$

$$+ k(J_s^2 - J_d^2)\cos(4\varphi_d)] \quad (A33)$$

where the canonical variables are

$$\varphi_s = \frac{1}{2}(\varphi_x + \varphi_y), \qquad J_s = I_x + I_y \quad (A34)$$

$$\varphi_d = \frac{1}{2}(\varphi_x - \varphi_y), \qquad J_d = I_x - I_y \quad (A35)$$

and

$$a_s = \frac{3}{8}\left(\frac{1}{\omega_{0x}^2} + \frac{1}{\omega_{0y}^2} + \frac{4}{3\omega_{0x}\omega_{0y}}\right) \qquad (A36)$$

$$a_d = \frac{3}{8}\left(\frac{1}{\omega_{0x}^2} + \frac{1}{\omega_{0y}^2} - \frac{4}{3\omega_{0x}\omega_{0y}}\right) \qquad (A37)$$

$$b = \frac{3}{4}\left(\frac{1}{\omega_{0x}^2} - \frac{1}{\omega_{0y}^2}\right) \qquad (A38)$$

$$k = \frac{1}{4}\frac{1}{\omega_{0x}\omega_{0y}}. \qquad (A39)$$

Since the Hamiltonian is independent on φ_s, it follows that J_s is a constant of motion.

The stable point (φ_d^*, J_d^*) is given by the equations $\dot{J}_d = 0$, $\dot{\varphi}_d = 0$ which lead to

$$\cos(4\varphi_d^*) = -1, \qquad J_d^* = \frac{\Delta\omega\bar{\omega}^2}{\alpha}, \qquad (A40)$$

up to the first order in $\Delta\omega$. The particle dynamics around the stable point is described by the effective Hamiltonian

$$H_{\text{eff}} = \frac{\alpha}{2\bar{\omega}^2}\delta J_d^2 + 2\frac{\alpha}{\bar{\omega}^2}(J_s^2 - J_d^{*2})\delta\varphi_d^2 \qquad (A41)$$

where $\delta J_d = J_d - J_d^*$, $\delta\varphi_d = \varphi_d - \varphi_d^*$. The oscillation frequency of J_d in the proximity of the coupling resonance stable point is therefore

$$\omega_t = \frac{2\alpha}{\bar{\omega}^2}\sqrt{(J_s^2 - J_d^{*2})}. \qquad (A42)$$

Considering that

$$\dot{\varphi}_s = 2\alpha(a_s + k\cos(4\varphi_d))J_s = 2\frac{\alpha}{\bar{\omega}^2}J_s \qquad (A43)$$

$$\dot{\varphi}_d = \frac{\alpha}{\bar{\omega}^2}\delta J_d \qquad (A44)$$

the particle tunes are

$$\omega_x \approx \dot{\Phi}_x = \dot{\varphi}_s + \dot{\varphi}_d + \bar{\omega} = 2\frac{\alpha}{\bar{\omega}^2}J_s + \bar{\omega} + \frac{\alpha}{\bar{\omega}^2}(J_d - J_d^*) \qquad (A45)$$

$$\omega_y \approx \dot{\Phi}_y = \dot{\varphi}_s - \dot{\varphi}_d + \bar{\omega} = 2\frac{\alpha}{\bar{\omega}^2}J_s + \bar{\omega} - \frac{\alpha}{\bar{\omega}^2}(J_d - J_d^*). \qquad (A46)$$

Note that in the frequency space the main spectral feature of the trapped particle resides on the line $\omega_x = \omega_y$. The oscillation of J_d yields satellite features spaced by harmonics of the trapping frequency ω_t.

The frequency shift is given by

$$\delta\omega_x(J_s, J_d) = \omega_{0x} - \omega_x = \Delta\omega + 2\frac{\alpha}{\bar{\omega}^2}J_s + \frac{\alpha}{\bar{\omega}^2}(J_d - J_d^*) \qquad (A47)$$

$$\delta\omega_y(J_s, J_d) = \omega_{0y} - \omega_y = -\Delta\omega + 2\frac{\alpha}{\bar{\omega}^2}J_s - \frac{\alpha}{\bar{\omega}^2}(J_d - J_d^*). \qquad (A48)$$

In the presence of a transverse mode, in the rigid-slice approximation, the space charge potential is

$$V(x, y) = \alpha((x - \bar{x})^2 + y^2)^2. \qquad (A49)$$

The calculation of the mode-particle coupling reduces to analyzing the force acting on the particle. The equation of motion reads,

$$\ddot{x} + \omega_{0x}^2 x = -4\alpha x(x^2 + y^2) + 12\alpha x^2\bar{x} + 4\alpha y^2\bar{x}. \qquad (A50)$$

The displacement $\bar{x}$ is small and does not affect the incoherent particle motions in the first order approximation. Equation (A50) yields the mode-particle coupling written in action-angle coordinates as

$$\begin{aligned}-K\bar{x} &= (12\alpha x^2 + 4\alpha y^2)\bar{x} \\ &= \left[12\alpha\frac{(J_s + J_d)}{\omega_{0x}}\sin^2\Phi_x + 4\alpha\frac{(J_s - J_d)}{\omega_{0y}}\sin^2\Phi_y\right]\bar{x} \\ &= 2\alpha J_s\left[\frac{3}{\omega_{0x}}(1 - \cos 2\Phi_x) + \frac{1}{\omega_{0y}}(1 - \cos 2\Phi_y)\right]\bar{x} \\ &\quad + 2\alpha J_d\left[\frac{3}{\omega_{0x}}(1 - \cos 2\Phi_x) - \frac{1}{\omega_{0y}}(1 - \cos 2\Phi_y)\right]\bar{x}.\end{aligned} \qquad (A51)$$

Because J_s is constant, the first term in the r.h.s. of Eq. (A51) is resonant with x when $\omega_x \approx \omega_y \approx \omega_c$, as expected by a conventional Landau damping mechanism. A similar reasoning with the one discussed in Appendix A 1 can be used to calculate the mode-particle coupling. However, when analyzing the terms resonant with x one has to take into account that, according to Eq. (A40), the trapped particles phases satisfy $2\Phi_x - 2\Phi_y = (2k + 1)\pi$. Doing that, one gets for the coupling term proportional to J_s,

$$K_1\bar{x} = -J_s\left(\frac{9\alpha}{\omega_{0x}} + \frac{\alpha}{\omega_{0y}}\right)\bar{x} \approx -\frac{10\alpha J_s}{\omega_{0x}}\bar{x}. \qquad (A52)$$

On the other hand, since J_d is oscillating with the frequency ω_t, the term in the r.h.s. of Eq. (A51) proportional to J_d is resonant with x when $\omega_x \approx \omega_y \approx \omega_c - \omega_t$. Assuming that $J_d = |J_d|\cos\omega_t t$, $\bar{x} = M\sin\omega_c t$ and $2\Phi_x - 2\Phi_y = (2k + 1)\pi$, the mode-particle coupling proportional to J_d can be written as

$$K_2 \bar{x} = -J_d \left(\frac{15\alpha}{2\omega_{0x}} - \frac{3\alpha}{2\omega_{0y}} \right) \bar{x} \approx -\frac{6\alpha J_d}{\omega_{0x}} \bar{x}. \qquad \text{(A53)}$$

The equation of motion in the proximity of the coupling resonance for our simplified Hamiltonian is

$$\ddot{x} + (\omega_{0x} - \delta\omega_x(J_s, J_d))^2 x = -(K_1 + K_2)\bar{x}$$
$$= \frac{10\alpha}{\omega_{0x}} J_s \bar{x} + \frac{6\alpha}{\omega_{0x}} J_d \bar{x}. \qquad \text{(A54)}$$

The equation (12) proposed to described the motion of particles in the proximity of coupling resonance in Sec. III is a generalization of Eq. (A54) to include higher order terms in the space charge potential and, as well, longitudinal degrees of freedom.

---

[1] L. Landau, Oscillations of electron plasma, J. Phys. USSR **10**, 25 (1946).

[2] J. Gareyte, J. P. Koutchouk, and F. Ruggiero, Report No. CERN-LHC-PROJECT-REPORT-091, 1997.

[3] M. Blaskiewicz, Fast head-tail instability with space charge, Phys. Rev. ST Accel. Beams **1**, 044201 (1998).

[4] A. Burov, Head-tail modes for strong space charge, Phys. Rev. ST Accel. Beams **12**, 044202 (2009); **12**, 109901(E) (2009).

[5] V. Balbekov, Transverse modes of a bunched beam with space charge dominated impedance, Phys. Rev. ST Accel. Beams **12**, 124402 (2009).

[6] V. Kornilov and O. Boine-Frankenheim, Transverse modes of a bunched beam with space charge dominated impedance, Phys. Rev. ST Accel. Beams **13**, 114201 (2010).

[7] V. Kornilov and O. Boine-Frankenheim, Thresholds of the Head-Tail Instability in Bunches with Space Charge, in *Proceedings of the 54th ICFA Advanced Beam Dynamics Workshop on High-Intensity, High Brightness and High Power Hadron Beams, East-Lansing, MI, USA* (2014), http://epaper.kek.jp/HB2014.

[8] A. Macridin, A. Burov, E. Stern, J. Amundson, and P. Spentzouris, Simulation of transverse modes with their intrinsic Landau damping for bunched beams in the presence of space charge, Phys. Rev. ST Accel. Beams **18**, 074401 (2015).

[9] Elias Metral, Ph.D. Thesis, CERN-THESIS, 1999-074.

[10] B. W. Montague, CERN Report No. 68-38, 1968.

[11] Synergia2, Accelerator Modeling, https://cdcvs.fnal.gov/redmine/projects/synergia2/wiki.

[12] J. Amundson, P. Spentzouris, J. Qiang, and R. Ryne, Synergia: An accelerator modeling tool with 3-D space charge, J. Comp. Physiol. **211**, 229 (2006).

[13] P. J. Schmid, Dynamic mode decomposition of numerical and experimental data, J. Fluid Mech. **656**, 5 (2010).

[14] C. W. Rowley, I. Mezić, S. Bagheri, P. Schlatter, and D. S. Henningson, Spectral analysis of nonlinear flows, J. Fluid Mech. **641**, 115 (2009).

[15] J. H. Tu, C. W. Rowley, D. M. Luchtenburg, S. L. Brunton, and J. N. Kutz, On dynamic mode decomposition: Theory and applications, J. Comp. Nonlin. Dyn. **1**, 391 (2014).

[16] K. K. Chen, J. H. Tu, and C. W. Rowley, Variants of dynamic mode decomposition: Boundary condition, koopman, and fourier analyses, J. Nonlinear Sci. **22**, 887 (2012).

[17] A. Chao, *Physics of Collective Beam Instabilities in High Energy Accelerators* (John Wiley & Sons, Inc., New York, 1993), Eq 5.2.

[18] D. Mohl and H. Schonauer, Landau damping by non-linear space-charge forces and octupoles, in *Proceedings of the IXth International Conference on High Energy Accelerators, Stanford* (Stanford Linear Accelerator Center, Stanford, 1974), p. 380, http://www.slac.stanford.edu/pubs/slacreports/reports16/slac-r-839-c.pdf.

[19] H. Yoshida, Construction of higher order symplectic integrators, Phys. Lett. A **150**, 262 (1990).

[20] R. W. Hockney and J. W. Eastwood, *Computer Simulation Using Particles* (McGraw-Hill, New York, 1981).

[21] See Ref. [15] and the references therein.

[22] B. W. Brunton, L. A. Johnson, J. G. Ojemann, and J. Nathan Kutz, Extracting spatial–temporal coherent patterns in large-scale neural recordings using dynamic mode decomposition, J. Neurosci. Methods **258**, 1 (2016).

[23] J. Grosek and J. Nathan Kutz, Dynamic mode decomposition for real-time background/foreground separation in video, arXiv:1404.7592.

[24] A. H. Nayfeh, *Perturbation Methods* (WILEY-VCH Valag GmbH & Co. KGaA, New York, 2000), ch. 3.1.1

[25] For the Landau damping mechanism only the part of the solution in phase with the driving force is relevant, see chapter 5 in [17].